Interference effect between ϕ and $\Lambda(1520)$ photoproduction channels at SPring-8/LEPS

S. Y. Ryu,[1] J. K. Ahn,[2] T. Nakano,[1] D. S. Ahn,[3] S. Ajimura,[1] H. Akimune,[4] Y. Asano,[5] W. C. Chang,[6] J. Y. Chen,[7] S. Daté,[8] H. Ejiri,[1] H. Fujimura,[9] M. Fujiwara,[1] S. Fukui,[1] S. Hasegawa,[1] K. Hicks,[10] K. Horie,[11] T. Hotta,[1] S. H. Hwang,[12] K. Imai,[13] T. Ishikawa,[14] T. Iwata,[15] Y. Kato,[16] H. Kawai,[17] K. Kino,[1] H. Kohri,[1] Y. Kon,[1] N. Kumagai,[8] P. J. Lin,[6] Y. Maeda,[18] S. Makino,[9] T. Matsuda,[19] N. Matsuoka,[1] T. Mibe,[20] M. Miyabe,[14] M. Miyachi,[21] Y. Morino,[20] N. Muramatsu,[14] R. Murayama,[11] Y. Nakatsugawa,[20] S. i. Nam,[22] M. Niiyama,[23] M. Nomachi,[1] Y. Ohashi,[8] H. Ohkuma,[8] T. Ohta,[1] T. Ooba,[17] D. S. Oshuev,[6] J. D. Parker,[23] C. Rangacharyulu,[24] A. Sakaguchi,[11] T. Sawada,[6] P. M. Shagin,[25] Y. Shiino,[17] H. Shimizu,[14] E. A. Strokovsky,[26,*] Y. Sugaya,[1] M. Sumihama,[27] A. O. Tokiyasu,[14] Y. Toi,[19] H. Toyokawa,[8] T. Tsunemi,[23] M. Uchida,[21] M. Ungaro,[28] A. Wakai,[29] C. W. Wang,[6] S. C. Wang,[6] K. Yonehara,[4] T. Yorita,[1] M. Yoshimura,[30] M. Yosoi,[1] and R. G. T. Zegers[31]

(The LEPS Collaboration)

[1]*Research Center for Nuclear Physics, Osaka University, Ibaraki, Osaka 567-0047, Japan*
[2]*Department of Physics, Korea University, Seoul 02841, Republic of Korea*
[3]*RIKEN, The Institute of Physical and Chemical Research, Wako, Saitama 351-0198, Japan*
[4]*Department of Physics, Konan University, Kobe, Hyogo 658-8501, Japan*
[5]*XFEL Project Head Office, RIKEN, Sayo, Hyogo 679-5143, Japan*
[6]*Institute of Physics, Academia Sinica, Taipei 11529, Taiwan*
[7]*Light Source Division, National Synchrotron Radiation Research Center, Hsinchu, 30076, Taiwan*
[8]*Japan Synchrotron Radiation Research Institute, Sayo, Hyogo 679-5143, Japan*
[9]*Wakayama Medical College, Wakayama, 641-8509, Japan*
[10]*Department of Physics and Astronomy, Ohio University, Athens, Ohio 45701, USA*
[11]*Department of Physics, Osaka University, Toyonaka, Osaka 560-0043, Japan*
[12]*Korea Research Insititute of Standards and Science (KRISS), Daejeon 34113, Republic of Korea*
[13]*Advanced Science Research Center, Japan Atomic Energy Agency, Tokai, Ibaraki 319-1195, Japan*
[14]*Research Center for Electron Photon Science, Tohoku University, Sendai, Miyagi 982-0826, Japan*
[15]*Department of Physics, Yamagata University, Yamagata 990-8560, Japan*
[16]*Kobayashi-Maskawa Institute, Nagoya University, Nagoya, Aichi 464-8602, Japan*
[17]*Department of Physics, Chiba University, Chiba 263-8522, Japan*
[18]*Proton Therapy Center, Fukui Prefectural Hospital, Fukui 910-8526, Japan*
[19]*Department of Applied Physics, Miyazaki University, Miyazaki 889-2192, Japan*
[20]*High Energy Accelerator Organization (KEK), Tsukuba, Ibaraki 305-0801, Japan*
[21]*Department of Physics, Tokyo Institute of Technology, Tokyo 152-8551, Japan*
[22]*Department of Physics, Pukyong National University, Busan 48513, Republic of Korea*
[23]*Department of Physics, Kyoto University, Kyoto 606-8502, Japan*
[24]*Department of Physics and Engineering Physics, University of Saskatchewan, Saskatoon, SK S7N 5E2, Canada*
[25]*School of Physics and Astronomy, University of Minnesota, Minneapolis, MN 55455, USA*
[26]*Joint Institute for Nuclear Research, Dubna, Moscow Region, 142281, Russia*
[27]*Department of Education, Gifu University, Gifu 501-1193, Japan*
[28]*Department of Physics, University of Connecticut, Storrs, CT 06269-3046, USA*
[29]*Akita Research Institute of Brain and Blood Vessels, Akita 010-0874, Japan*
[30]*Institute for Protein Research, Osaka University, Suita, Osaka 565-0871, Japan*
[31]*National Superconducting Cyclotron Laboratory, Michigan State University, East Lansing, MI 48824, USA*

The ϕ-meson production has the unique feature within gluon dynamics of being a result of OZI suppression due to the dominant $s\bar{s}$ structure of the ϕ meson, which is predicted to proceed via a Pomeron trajectory with $J^{PC} = 0^{++}$ [1–7]. Cross sections for diffractive ϕ photoproduction are then predicted to increase smoothly with photon energy. However, a bump structure at $\sqrt{s} = 2.1$ GeV in forward differential cross sections was first reported by the LEPS collaboration [8].

Despite extensive experimental efforts devoted for the photoproduction of ϕ mesons near threshold, the nature of the bump structure has not yet been explained in detail [9, 10]. Kiswandhi *et al.* [11] suggested that the bump structure is the result of an excitation of missing nucleon resonances. However, the bump structure observed from CLAS appears only at forward angles; thus, a conventional resonance interpretation seems less likely [10].

*Research Center for Nuclear Physics, Osaka University, Ibaraki, Osaka 567-0047, Japan

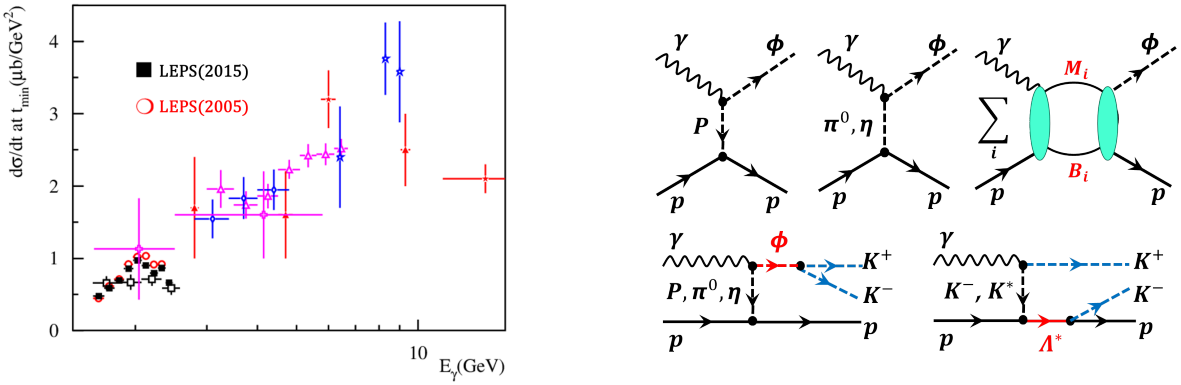

FIG. 1: (Left) Forward differential cross sections for ϕ photoproduction near threshold. (Right-top) Dominant diagrams for photoproduction of ϕ meson from proton. (Right-bottom) Photoproduction of K^-K^+p via ϕ and $\Lambda(1520)$ resonances produced by Pomeron and K/K^* exchanges, respectively.

Very recently, the LHCb collaboration [12] claimed to have observed two J/ψ p resonances referred to as hidden-charm pentaquark states ($c\bar{c}uud$) from Λ_b^0 decays. In ϕ photoproduction, a hidden-strangeness pentaquark state could also be searched for as a candidate for the forward bump structure. Recent theoretical studies further relate this to a coupling between the ϕp and $K^+\Lambda(1520)$ channels, because the bump structure occurs very close to the threshold of $\Lambda(1520)$ production [13, 14]. The ϕ-$\Lambda(1520)$ interference could also account for the bump structure, but it has not yet been measured in K^+K^-p photoproduction. The interference may be either positive (constructive) or negative (destructive), depending on the relative phase between the amplitudes of ϕ and $\Lambda(1520)$ production.

Here, we report on the measurement of forward differential cross sections for ϕ and $\Lambda(1520)$ photoproduction and the relative phase angles between their photoproduction amplitudes. This analysis includes the event selection for $\gamma p \to K^+K^-p$, which was based on a kinematic fit. The yields of ϕ and $\Lambda(1520)$ were obtained from a simultaneous fit of the $m_{K^+K^-}$ and m_{K^-p} invariant masses with lineshapes from a Monte-Carlo simulation. This self-consistent analysis enables the investigation of interference effects between ϕ and $\Lambda(1520)$. To our knowledge, no interference measurement for this reaction has previously been reported in the literature. The experiment was carried out using the

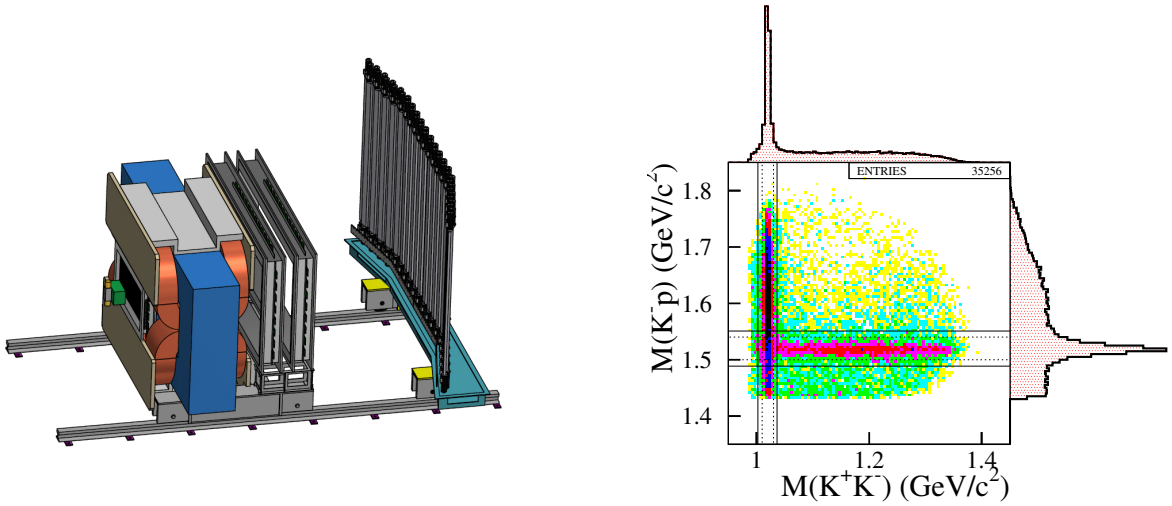

FIG. 2: (Left) Schematic view of the LEPS spectrometer at SPring-8; (Right) A scatter plot of the reconstructed masses for K^-K^+ and K^-p systems. The projections onto each invariant mass axis are shown as histograms on the top and right sides.

LEPS detector at the SPring-8 facility. Linearly polarized photons with energies from 1.5 to 2.4 GeV were produced using a laser backscattering technique [15] with UV lasers. The photon beam was incident on a 15-cm liquid-hydrogen (LH_2) target, in which K^+, K^- and p particles were produced and then passed through the LEPS spectrometer with the standard configuration [16]. With a full data set of LH_2 runs, an analysis on ϕ-$\Lambda(1520)$ photoproduction was performed using kinematic fits and simultaneous fits on the K^+K^- and K^-p mass spectra with Monte-Carlo

lineshapes. To identify candidate events, at least two of the K^+, K^-, and p tracks were required to be reconstructed using standard particle identification methods.

Forward particle pairs correspond to the pairs mostly produced in the range of $\cos\theta^* > 0.5$, where θ^* is the angle between the pair and the beam axis in the production center of mass system. The kinematic fit reconstructs three unmeasured parameters for a missing particle in the K^-K^+p final state. The energy and momentum conservation laws provide four constraints. Consequently, we have an overdetermined system with four constraints and three unknowns.

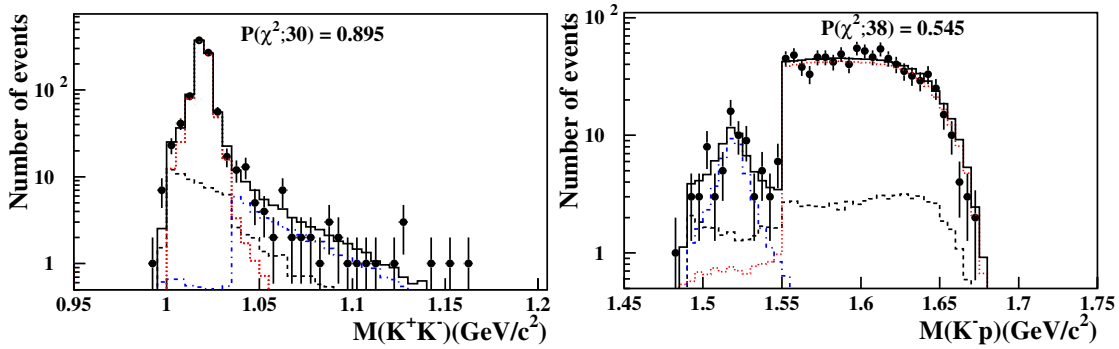

FIG. 3: The invariant mass spectra for (top) K^+K^- and (bottom) K^-p systems are displayed as closed circles for forward K^+K^- events in the energy region from 1.973 to 2.073 GeV, respectively. The best-fit lineshapes for ϕ are overlaid with dotted lines, while those for $\Lambda(1520)$ are represented as dot-dashed lines. Dashed lines represent the contributions of non-resonant K^+K^-p production.

The measured K^+K^- and K^-p mass spectra for the selected K^+K^-p events were fitted with lineshapes from simulated processes of the ϕp [18], $\Lambda(1520)K^+$ [19], and non-resonant K^+K^-p channels. For events in which K^+p is detected, these mass spectra are fitted with the three processes as well as $K^{*0}\Sigma^+$ [20] and $K^+(\Lambda(1520) \to \Sigma^+\pi^-)$. The best-fit lineshapes for ϕ, $\Lambda(1520)$ and non-resonant K^+K^-p well reproduce the K^+K^- and the K^-p mass spectra, as shown in Fig. 3. The fits with Monte-Carlo lineshapes were based on the events beyond the ϕ-$\Lambda(1520)$ interference region in which the two resonances appear. The fit results were then interpolated into the interference region, keeping the magnitudes of Monte-Carlo lineshapes as determined from the fit [21]. This simultaneous fit with Monte-Carlo lineshapes is a self-consistent method to reproduce the measured K^+K^- and K^-p mass spectra, which pertains to the further study of interference effects.

Forward differential cross sections for ϕ and $\Lambda(1520)$ production channels were measured using the best-fit results with Monte-Carlo lineshapes in the ϕ and $\Lambda(1520)$ mass bands except for the interference region. We reconfirmed the existence of the bump structure around $E_\gamma = 2.0$ GeV. The structure appears persistent even with different ϕ-mass bands, different slope parameters, and the exclusion of the interference region in which ϕ and $\Lambda(1520)$ mass bands overlap. The slope parameters of the $|t - t_{\rm min}|$ distributions decreased as the photon energy increased. The differential cross sections for $\Lambda(1520)$ photoproduction in the angular regions of $0.9 < \cos\theta^*_{K^+} < 1.0$ are compared with the previous LEPS results by Kohri *et al.* [22]. While the previous analysis was based on events with a single K^+ track, the new analysis required at least two tracks among K^-, K^+, and p. Though the statistics were low, both results are in good agreement with the earlier analysis and feature the bump structure near $E_\gamma = 2$ GeV. Interestingly, the two cross-section results show the bump structure at the same E_γ, which could indicate a strong correlation between the ϕ and $\Lambda(1520)$. However, the difference between the cross sections obtained with and without the interference region is not large enough to account for the bump structure.

The differential cross sections for the $\gamma p \to K^+K^-p$ reaction can be decomposed into

$$\frac{d^2\sigma}{dm_{K^+K^-}dm_{K^-p}} \propto |\mathcal{M}_\phi + \mathcal{M}_{\Lambda(1520)} + \mathcal{M}_{\rm nr}|^2, \tag{1}$$

where $\mathcal{M}_\phi$ and $\mathcal{M}_{\Lambda(1520)}$ are the complex amplitudes for ϕ and $\Lambda(1520)$ production processes, respectively. $\mathcal{M}_{\rm nr}$ represents non-resonant K^+K^-p production. Each complex amplitude includes individual amplitudes for all possible sub-processes, such as Pomeron-exchange and pseudoscalar meson-exchange processes for ϕ photoproduction. However, log-likelihood fits of the data in ϕ and $\Lambda(1520)$ bands excluding the ϕ and $\Lambda(1520)$ interference region ($|\mathcal{M}_\phi + \mathcal{M}_{\rm nr}|^2$) with Monte-Carlo lineshapes ($|\mathcal{M}_\phi|^2 + |\mathcal{M}_{\rm nr}|^2$) result in the χ^2 probability $P(\chi^2) > 0.2$ in most cases. Moreover, the S-P wave interference in ϕ photoproduction is known to be as small as 1% [23]. Therefore, we assume that $|\mathcal{M}_\phi + \mathcal{M}_{\Lambda(1520)} + \mathcal{M}_{\rm nr}|^2 \approx |\mathcal{M}_\phi + \mathcal{M}_{\Lambda(1520)}|^2 + |\mathcal{M}_{\rm nr}|^2$, where the interference terms between $\mathcal{M}_{\rm nr}$ and two resonance amplitudes are neglected. The contribution from the term $|\mathcal{M}_{\rm nr}|^2$ was then subtracted from the data.

The differential cross sections for the $\gamma p \to K^+K^-p$ reaction via the ϕ and $\Lambda(1520)$ resonances can be written as [24]

$$\left.\frac{\mathrm{d}^2\sigma}{\mathrm{d}m_{K^+K^-}\mathrm{d}m_{K^-p}}\right|_{\phi,\Lambda(1520)} \propto |\mathcal{M}_\phi + \mathcal{M}_{\Lambda(1520)}|^2 = \left|\frac{a\ e^{i\psi_a}}{m_\phi^2 - m^2_{K^+K^-} + im_\phi\Gamma_\phi} + \frac{b\ e^{i\psi_b}}{m^2_{\Lambda^*} - m^2_{K^-p} + im_{\Lambda^*}\Gamma_{\Lambda^*}}\right|^2, \quad (2)$$

where a and b denote the magnitudes of the Breit-Wigner amplitudes for ϕ and $\Lambda(1520)$, respectively. Here ψ_a and ψ_b represent phases for ϕ and $\Lambda(1520)$ production amplitudes, respectively. We integrate the differential cross sections over the K^-p mass interval in the ϕ-$\Lambda(1520)$ interference region, assuming that the phase ψ_b is constant in the interference region for each energy interval. The integrated cross sections can then be given by

$$\frac{\mathrm{d}\sigma}{\mathrm{d}m} \propto \left|\frac{a\ e^{i\psi_a}}{m_\phi^2 - m^2 + im_\phi\Gamma_\phi} + B(m)e^{i\psi_b}\right|^2, \quad (3)$$

where m denotes $m_{K^+K^-}$. $|B(m)|^2$ corresponds to the Breit-Wigner lineshape of $\Lambda(1520)$ projected onto the K^+K^- mass axis in the interference region. The interference term $I(m)$ between the two amplitude terms can be obtained as [25]

$$I(m) = 2|aB(m)|\frac{(m_\phi^2 - m^2)\cos\psi + \Gamma_\phi m_\phi \sin\psi}{(m_\phi^2 - m^2)^2 + m_\phi^2\Gamma_\phi^2}, \quad (4)$$

where $\psi = |\psi_a - \psi_b|$ is the relative phase between the phases, ψ_a and ψ_b.

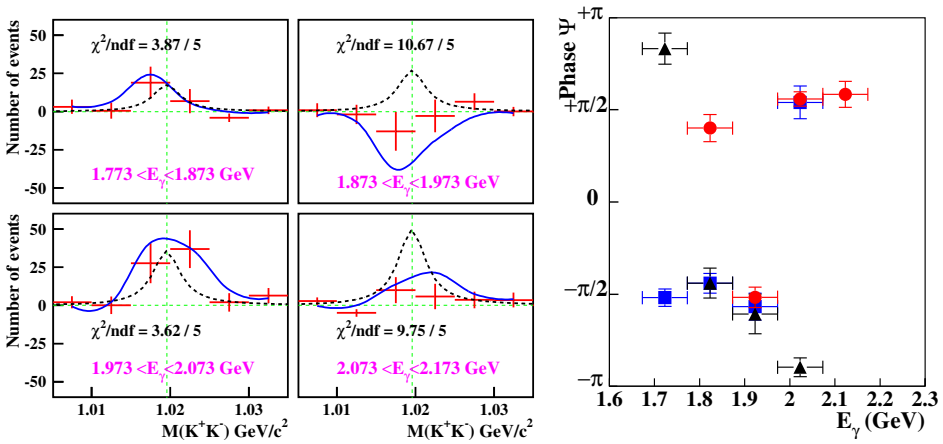

FIG. 4: (Left) Difference between event yields in the interference region and the sum of ϕ and $\Lambda(1520)$ events for forward K^+K^- events, in four 0.1-GeV wide energy regions from 1.773 GeV to 2.173 GeV. The best-fit results for the relative phase are overlaid with solid curves, while dashed lines are from theoretical estimates assuming maximum constructive ϕ-$\Lambda(1520)$ interference with $\psi = \pi/2$. (Right) Phase angles for K^+K^- (circles), K^-p (squares), and K^+p (triangles) events.

For the relative phase between the ϕ and $\Lambda(1520)$ amplitudes, we fitted data in the interference region with Eq. 4. Here, the relative amplitudes of a and $B(m)$ for each energy interval are fixed from a simultaneous fit utilizing Monte-Carlo lineshapes in the ϕ and $\Lambda(1520)$ mass bands except for the interference region. Consequently, only a single parameter, the relative phase ψ, exists in the fit. The best-fit results for the relative phase are shown as solid curves in Fig. 4. To verify the reliability of this approach, the fit results are compared with theoretical estimates based on the effective Lagrangian approach [26], taking the ϕ and $\Lambda(1520)$ production amplitudes into account. The reaction dynamics is represented by the invariant amplitudes and form factors in this theoretical approach. The phase of $\psi = \pi/2$ was chosen for simplicity. The theoretical estimates for the maximum constructive ϕ-$\Lambda(1520)$ interference are shown as dashed curves in Fig. 4, which are consistent with those predicted by Eq. 4.

The fit results for relative phase are represented in Fig. 4(right). The χ^2 probability was required to exceed 0.1%. For forward K^-p and K^+p events, the energy regions between 1.673 GeV and 2.073 GeV are explored. The maximum constructive interference has $\psi = \pi/2$, while the maximum destructive interference is represented by $\psi = -\pi/2$. For

K^+K^- events detected in the forward directions, the resulting relative phases are in most cases constructive, while those for forward $K^\pm p$ events are destructive.

For forward K^+K^- events in the energy region of $1.973 < E_\gamma < 2.073$ GeV, the integrated event yield in the interference region approaches close to the maximum bound for the ϕ-Λ interference, which is consistent with the relative phase $\psi = 1.69 \pm 0.12$ rad. Moreover, the relative phase flips its sign as a function of photon energy E_γ. For K^-p events, the relative phase in the energy region of $1.973 < E_\gamma < 2.073$ GeV firmly stays at a positive value, while in other energy regions it supports destructive interference. Thus, it can be inferred that a change in interference patterns occurs when K^-p is studied at forward angles. For the K^+p events, only in the lowest-energy region does the phase appears in the positive side, but it remains close to π, which corresponds to zero interference.

Different phases for different event modes (forward K^+K^-, K^-p and K^+p events) may arise from differing kinematic coverages for the photoproduction of ϕ and $\Lambda(1520)$. We relate the phases near $\pi/2$ for forward K^+K^- events to the interference between the Pomeron exchange amplitude for ϕ and the K-exchange amplitude for $\Lambda(1520)$ photoproduction. For forward proton events (K^-p and K^+p), unnatural-parity exchange processes become important in ϕ photoproduction. However, it is worth noting that the ϕ-$\Lambda(1520)$ interference effect does not account for the 2.1-GeV bump structure in forward differential cross sections for ϕ photoproduction. This result is consistent with a recent report from CLAS regarding the $\Lambda(1520)$ effect [10]. The energy dependence of the phase may indicate nontrivial rescattering contributions from other hyperon resonances. The bump structure could then be associated with either rescattering processes due to kinematic overlap in phase space or exotic structures involving a hidden-strangeness pentaquark state and the exchange of a new Pomeron. Alternatively, they could be due to a combination of both factors.

In summary, the photoproduction of the $\gamma p \to K^+K^-p$ reaction was measured using the LEPS detector at energies from 1.57 to 2.40 GeV. The ϕ-$\Lambda(1520)$ interference measurement is a good probe to study the origin of enhanced production cross sections for ϕ and $\Lambda(1520)$ near $\sqrt{s} = 2.1$ GeV. We reconfirmed the bump structure in the analysis without the ϕ-$\Lambda(1520)$ interference region. On the other hand, we observed clear ϕ-$\Lambda(1520)$ interference effects in the energy range from 1.673 to 2.173 GeV. The data obtained in the present study provide the first-ever experimental evidence for the ϕ-$\Lambda(1520)$ interference effect in ϕ photoproduction. The relative phases suggest strong constructive interference for K^+K^- pairs observed at forward angles, while destructive interference results from the emission of protons at forward angles. The nature of the bump structure could originate from interesting exotic structures such as a hidden-strangeness pentaquark state, a new Pomeron exchange and rescattering processes via other hyperon states.

[1] A. I. Titov, T.-S. H. Lee, H. Toki, and O. Streltsova, Phys. Rev. C **60**, 035205 (1999).
[2] A. I. Titov, T. Nakano, S. Daté and Y. Ohashi, Mod. Phys. Lett. A **23**, 2301 (2008).
[3] D. Schildknecht, Acta Physica Polonica B **37**, 595 (2006).
[4] A. Sibirtsev, H. W. Hammer, U. G. Meissner, and A.W. Thomas, Eur. Phys. J. A **29**, 209 (2006).
[5] J.-M. Laget, Phys. Lett. B **489**, 313 (2000).
[6] A. Donnachie, H. G. Dosch, P. V. Landshoff and O. Natchmann, Pomeron Physics and QCD, Cambridge University Press (2002).
[7] A. Donnachie and P. V. Landshoff, Nucl. Phys. B **244**, 322 (1984).
[8] T. Mibe *et al.* (LEPS Collaboration), Phys. Rev. Lett. **95**, 182001 (2005).
[9] H. Seraydaryan *et al.* (CLAS Collaboration), Phys. Rev. C **89**, 055206 (2014).
[10] B. Dey *et al.* (CLAS Collaboration), Phys. Rev. C **89**, 055208 (2014).
[11] A. Kishwandhi *et al.*, Phys. Lett. B **691**, 214 (2010).
[12] R. Aaij *et al.* (LHCb Collaboration), Phys. Rev. Lett. **115**, 072001 (2015).
[13] S. Ozaki, A. Hosaka, H. Nagahiro, and O. Scholten, Phys. Rev. C **80**, 035201 (2009).
[14] H-Y. Ryu, A. I. Titov, A. Hosaka, and H-Ch. Kim, Prog. Theor. Exp. Phys. **2014**, 023D03 (2014).
[15] N. Muramatsu *et al.*, Nucl. Instrum. Methods A **737**, 184 (2014).
[16] T. Nakano *et al.*, Nucl. Phys. A **670**, 332 (2000); *ibid*, A **721**, 112 (2003).
[17] K. A. Olive *et al.* (Particle Data Group), Chin. Phys. C, **38**, 090001 (2014).
[18] W. C. Chang *et al.*, Phys. Rev. C **82**, 015205 (2010).
[19] J. Y. Chen, Ph.D. thesis, National Sun Yat-sen University, 2009.
[20] S. H. Hwang *et al.* (LEPS Collaboration), Phys. Rev. Lett. **108**, 092001 (2012).
[21] S. Y. Ryu, Ph.D. thesis, Osaka University, 2015.
[22] H. Kohri *et al.* (LEPS Collaboration), Phys. Rev. Lett. **104**, 172001 (2010).
[23] D. C. Fries *et al.*, Nucl. Phys. B **143**, 408 (1978).
[24] H. Ejiri *et al.*, Phys. Rev. Lett. **21**, 373 (1968); H. Ejiri and J. P. Bondorf, Phys. Lett. B **28**, 304 (1968); H. Ejiri *et al.*, Nucl. Phys. A **128**, 388 (1969).
[25] Y. Azimov, J. Phys. G: Nucl. Part. Phys. **37**, 023001 (2010).
[26] S. i. Nam *et al.*, the theoretical calculation approach will be published elsewhere.